

The radial distribution of blue straggler stars and the nature of their progenitors

M. Mapelli¹, S. Sigurdsson², F. R. Ferraro³, M. Colpi⁴, A. Possenti⁵, B. Lanzoni⁶

¹*S.I.S.S.A., Via Beirut 2 - 4, I-34014 Trieste, Italy; mapelli@sissa.it*

²*Department of Astronomy and Astrophysics, The Pennsylvania State University, 525 Davey Lab, University Park, PA 16802*

³*Dipartimento di Astronomia, Università di Bologna, via Ranzani 1, I-40126 Bologna, Italy*

⁴*Dipartimento di Fisica G. Occhialini, Università di Milano Bicocca, Piazza della Scienza 3. I-20126 Milano, Italy*

⁵*INAF, Osservatorio Astronomico di Cagliari, Poggio dei Pini, Strada 54, I-09012 Capoterra, Italy*

⁶*INAF, Osservatorio Astronomico di Bologna, via Ranzani 1, I-40126 Bologna, Italy*

7 February 2020

ABSTRACT

The origin of blue straggler stars (BSS) in globular clusters (GCs) is still not fully understood: they can form from stellar collisions, or through mass-transfer in isolated, primordial binaries (PBs). In this paper we use the radial distribution of BSS observed in four GCs (M3, 47 Tuc, NGC 6752 and ω Cen) to investigate which formation process prevails. We find that both channels coexist in all the considered GCs. The fraction of mass-transfer (collisional) BSS with respect to the total number of BSS is around $\sim 0.4 - 0.5$ ($\sim 0.5 - 0.6$) in M3, 47 Tuc, and NGC 6752. The case of ω Cen is peculiar with an underproduction of collisional BSS. The relative lack of collisional BSS in ω Cen can be understood if mass segregation has not yet driven to the core a sizeable number of PBs, which dominate stellar collisions through three and four-body processes. The spatial distribution of BSS provides strong hints to their origin: the BSS in the cluster outskirts form almost exclusively from mass-transfer in PBs, whereas the BSS found close to the cluster core most likely have a collisional origin.

Key words: stellar dynamics - binaries : general - blue stragglers - globular clusters: individual (M3, 47 Tuc, NGC 6752, ω Cen)

1 INTRODUCTION

Blue straggler stars (BSS) are stars lying above and blue-ward of the turn-off in the color-magnitude diagram (CMD) of a star cluster. At least two different processes have been proposed to explain their formation (Fusi Pecci et al. 1992; Bailyn 1995; Bailyn and Pinsonneault 1995; Proctor Sills, Bailyn & Demarque 1995; Sills & Bailyn 1999; Sills et al. 2000; Hurley et al. 2001). The first, dubbed the *mass-transfer scenario*, suggests that BSS are generated by primordial binaries (hereafter PBs) that evolve mainly in isolation until they start mass-transfer and possibly coalesce (McCrea 1964; Carney et al. 2001). The second, known as the *collisional scenario*, states that BSS are the product of a merger between two main sequence stars (MSs) in a dynamical interaction that involves a MS-MS collision, most likely in a binary-MS encounter (Davies, Benz & Hills 1994; Lombardi et al. 2002). The collisional BSS (COL-BSS) differ kinematically from the mass-transfer BSS (MT-BSS), since they are believed to acquire kicks due to dynamical recoil. In both these hypotheses, the resulting BSS have mass exceeding the turn-off mass of the cluster and are fueled by

hydrogen thanks to the mixing of the hydrogen-rich surface layers of the two progenitor stars.

The two aforementioned scenarios do not necessarily exclude each other and might coexist within the same star cluster (Ferraro et al. 1993; Davies, Piotto & De Angeli 2004; Mapelli et al. 2004). However, until recently, it has been difficult to estimate the relative importance of the two formation channels in a given globular cluster (GC). A new approach to solve this problem has been presented by Mapelli et al. (2004; hereafter paper I), who revised and upgraded an original attempt by Sigurdsson, Davies & Bolte (1994). The basic input for the new method is the observation of the shape of the BSS radial distribution in a star cluster. After the pioneering works on M3 (Ferraro et al. 1993; Ferraro et al. 1997a) and M55 (Zaggia et al. 1997), accurate determinations of the spatial distribution of BSS are now being obtained for an increasing sample of GCs (Ferraro et al. 2004 for 47 Tuc; Sabbi et al. 2004 for NGC 6752; Ferraro et al. 2006a for ω Cen; Warren, Sandquist & Bolte 2006 for M5). A very interesting result is emerging from these observations: BSS display a clear tendency to follow a bimodal

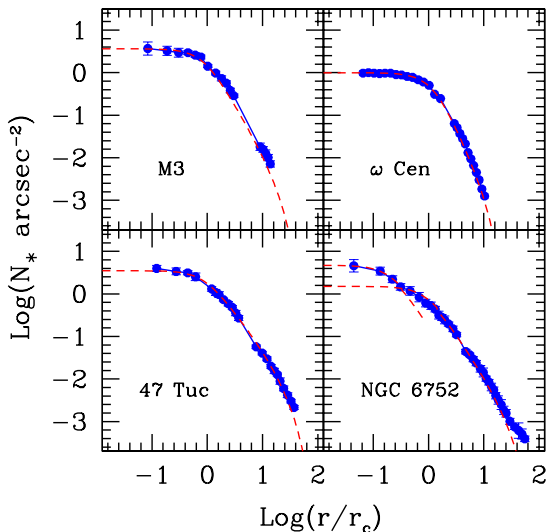


Figure 1. Comparison between the observed surface star density profile of the considered GCs (solid line and full circles) and the adopted multi-mass King model (dashed line). The units on the y-axis are number of stars per arcsec². The observed profiles are taken from Ferraro et al. (1997a) for M3, Ferraro et al. (2006a) for ω Cen, Mapelli et al. (2004) for 47 Tuc, Ferraro et al. (2003b) for NGC 6752.

spatial distribution, with a peak in the core, decreasing at intermediate radii and rising again at larger radii.

In paper I, Mapelli et al. focused on 47 Tuc and showed that the bimodal distribution can be reproduced assuming a suitable combination of the two proposed mechanisms for forming BSS. In particular, it was suggested (paper I) that the BSS in the core of 47 Tuc are mainly COL-BSS, while the external BSS are MT-BSS. This result agrees with studies of the BSS luminosity function in 47 Tuc (Bailyn & Pinsonneault 1995; Sills & Bailyn 1999; Sills et al. 2000; Ferraro et al. 2003a; Monkman et al. 2006).

In this paper, we explore two other GCs, whose BSS have a bimodal radial distribution. The aim is to test whether the conclusions drawn for 47 Tuc can be extended to GCs having different mass, concentration, central density, and velocity dispersion with respect to 47 Tuc. In particular, we study whether the position of a BSS in a GC can reliably be regarded as a signature for its origin. We also consider the case of ω Cen, whose radial distribution of BSS is flat. We follow the same procedure of paper I, carrying out dynamical simulations of BSS evolved in the gravitational potential well of their associated cluster. Details about the simulations are illustrated in Section 2; the sample of the investigated clusters is presented in Section 3. The results for M3, NGC 6752 and 47 Tuc are discussed in Section 4, whilst Section 5 is devoted to the outlier, ω Cen. In Section 6 we discuss our findings in comparison with the findings of Davies et al. (2004). Finally in Section 7 we present our conclusions.

2 THE SIMULATIONS

The simulations have been performed with an upgraded version (fully described in paper I) of the code originally developed by Sigurdsson & Phinney (1995). This code follows the dynamical evolution of a BSS in a static cluster background, which is modeled using a multi-mass King density profile. In this case, once the classes of mass have been selected, the cluster background is uniquely determined by imposing a central velocity dispersion σ , a core stellar density n_c and a dimensionless central potential W_0 ($W_0 \equiv \Psi(0)/\langle \sigma \rangle^2$, where $\langle \sigma \rangle$ is the mean core velocity dispersion and $\Psi(0) \equiv \Phi(r_t) - \Phi(0)$, with $\Phi(r)$ the gravitational potential at the radius r and r_t the tidal radius). In practice, we have chosen 10 classes of mass (the same classes reported in Table 1 of paper I) and have adopted the best available estimates of σ and n_c for each of the considered clusters. The values of W_0 for each GC have been derived by fitting the simulated star density profile to the observed one (see Section 3 and Table 1 for details).

Once the background has been determined, the dynamical evolution of the current population of BSS is simulated assuming a value for the ratio between the number of MT-BSS and that of COL-BSS. As far as the birth places are concerned, we assume that COL-BSS are generated exclusively in the innermost region, within the core radius (r_c), where the star density highest, leading to a high collision rate (Leonard 1989; Pooley et al. 2003). MT-BSS can be generated everywhere in the cluster, but are expected to be more frequent in the peripheral regions, where PBs can evolve in isolation, without suffering exchange or ionization by gravitational encounters (Sigurdsson & Phinney 1993; Ivanova et al. 2004). For this reason, in our simulations the MT-BSS, formed in PBs, are generated outside the cluster core with initial locations distributed in several radial intervals, between 1 and $80 r_c$. Within this region, all initial positions are randomly chosen following a flat probability distribution, according to the fact that the number of stars N in a King model scales as $dN = n(r) dV \propto r^{-2} \pi r^2 dr \propto dr$.

BSS velocities are randomly generated following the distribution illustrated in Section 3 of Sigurdsson & Phinney 1995 (eq. 3.3). In addition, we assign a natal kick velocity v_{kick} equal to $1 \times \sigma$ to those BSS formed collisionally in the core. We tried also different values of v_{kick} . In agreement with paper I, we find that v_{kick} higher than $2 - 3 \times \sigma$ causes the ejection of most of the BSS from the cluster, while there are no significant differences in the results for kick velocities ranging between 0 and $2 \times \sigma$. The masses of the BSS range between 1.2 and $1.5 M_{\odot}$. In paper I, we extended our analysis up to a mass of $2 M_{\odot}$ (Ferraro et al. 1997a; Gilliland et al. 1998); but now more stringent constraints are coming from observations (e.g. the upper limit for the mass of BSS in ω Cen is $1.4 M_{\odot}$; Ferraro et al. 2006a). On the other hand, in paper I we found that there is not significant difference between the behaviour of a 1.2 and a $2 M_{\odot}$ BSS. Each single BSS is evolved for a time $t_i = f_i t_{\text{last}}$, where f_i is a random number uniformly generated in $[0, 1]$ and t_{last} is the maximum lifetime attributed to a BSS. Given the uncertainty on the value of t_{last} , we have performed various sets of runs with t_{last} spanning the range between 1 and 5 Gyr. Consistent with the results of paper I, the best fits are all obtained for $t_{\text{last}} = 1.5$ Gyr. For 1 Gyr $\lesssim t_{\text{last}} \lesssim 2$ Gyr

Table 1. Globular cluster parameters

	r_c (pc)	σ (km s $^{-1}$)	n_c (stars pc $^{-3}$)	W_0	c	references ^a
NGC 104 (47 Tuc)	0.47	10	2.5×10^5	12	1.95	1, 2
NGC 5272 (M3)	1.5	4.8	6×10^3	10	1.77	1, 3
NGC 6752	0.1, 0.58 ^b	4.9, 12.4 ^c	2×10^5	13, 12 ^b	2.03, 1.95 ^b	1, 4
NGC 5139 (ω Cen)	4.1	17	5.6×10^3	6.5	1.40	5

^aReferences: 1 Dubath et al. 1997; 2 Mapelli et al. 2004; 3 Sigurdsson et al. 1994; 4 Drukier et al. 2003; 5 Merritt, Meylan & Mayor 1997.

^bThe double value of W_0 and c for NGC 6752 is due to the fact that the profile of this cluster is fit with a double King model. $W_0 = 13$ and $c = 2.03$ refer to the inner King (with core radius $5.7'' = 0.1$ pc for a distance of 4.3 kpc from the Sun; Ferraro et al. 2003b); while $W_0 = 12$ and $c = 1.95$ refer to the outer King (with core radius $28'' = 0.58$ pc; Ferraro et al. 2003b).

^cThe double value of σ for NGC 6752 refers to the two measurements $\sigma = 4.9^{+2.4}_{-1.4}$ km s $^{-1}$ (Dubath et al. 1997) and $\sigma = 12.4 \pm 0.5$ km s $^{-1}$ (Drukier et al. 2003).

the distribution does not change dramatically. If we choose a longer lifetime (3 Gyr or more), the dynamical friction washes out any peak of peripheral BSS; whereas for shorter lifetimes (less than 1 Gyr) any BSS could be hardly observable today.

Our code follows the dynamical evolution of the BSS in the cluster potential, subject to the action of dynamical friction and to the effects of distant encounters (eq. [3.4] of Sigurdsson and Phinney 1995).

The final positions of the BSS in each run determine the simulated radial distribution, to be compared with the observed one. We ran 10000 experiments for each of the considered cases. Since we studied ~ 10 different cases for each cluster, we made about ~ 400000 runs in total.

3 THE SAMPLE OF GLOBULAR CLUSTERS

We have studied the distribution of BSS in four different GCs: M3, 47 Tuc, NGC 6752 and ω Cen. They represent a very inhomogeneous sample of GCs. M3 is an intermediate density (6×10^3 stars pc $^{-3}$; Sigurdsson, Davies & Bolte 1994), low velocity dispersion (4.8 km s $^{-1}$; Dubath, Meylan & Mayor 1997) cluster. 47 Tuc and NGC 6752 are two very concentrated, maybe core collapsed clusters. ω Cen is the most massive among the Galactic GCs (5×10^6 M $_{\odot}$; Pryor & Meylan 1993; Meylan et al. 1995) and it is still a matter of debate whether it is a GC or the remnant of a dwarf galaxy (Zinnecker et al. 1988; Freeman 1993; Ideta & Makino 2004): it is a very loose cluster, with a wide metallicity spread and a clear evidence for rotation (van Leeuwen et al. 2000; Reijns et al. 2006; van de Ven et al. 2006).

The first step of our work consisted in finding the best match between the simulated star density profile of each cluster and the observed one. The results are shown in Fig. 1. The data of the star density profile of M3, NGC 6752 and ω Cen are from Ferraro et al. (1997a), Ferraro et al. (2003b) and Ferraro et al. (2006a), respectively. The star density profile of 47 Tuc is the same published in paper I. Note that we fit the profile of NGC 6752 with a double King model, as in Ferraro et al. (2003b). The adopted values of σ and n_c , and the fit values of W_0 are given in Table 1, as well as the concentration parameter c (where $c = \log(r_t/r_c)$) and the fiducial values of r_c in parsec. The latter quantities are derived by assuming a distance from the Sun of 4.6 kpc (47 Tuc, Ferraro et al. 1999, see also Table 3 by Beccari et al. 2006), 10.1

kpc (M3, Ferraro et al. 1999), 4.3 kpc (NGC 6752, Ferraro et al. 1999) and 5.5 kpc (ω Cen, Bellazzini et al. 2004).

The data for the radial distribution of BSS are taken from Ferraro et al. (1997a) for M3, Ferraro et al. (2004) for 47 Tuc, Sabbi et al. (2004) for NGC 6752 and Ferraro et al. (2006a) for ω Cen. As usual, the number of BSS is normalized to the number of red giant branch (RGB) stars or to the number of horizontal branch (HB) stars. Even if the considered GCs are very different from each other, the observed radial distributions of BSS are similar (see Fig. 2), with the exception of ω Cen. In fact, the radial distribution of BSS displays a maximum in the central region of the GC, decreases down to a minimum at intermediate radii (of order $5 r_c - 10 r_c$) and increases again at outer radii. ω Cen differs as it shows an almost flat distribution.

4 RESULTS AND DISCUSSION FOR M3, 47 TUC AND NGC 6752

We have explored whether the radial distribution of BSS observed in our sample of GCs can be reproduced with a model which predicts two different classes of progenitors for the BSS: (i) PBs evolved in isolation and (ii) binary (or single) stars which underwent collisions in the high density environment of the GC core. Fig. 2 shows the results obtained for M3, 47 Tuc, NGC 6752 and ω Cen. In all cases, our adopted model provides a statistically acceptable fit to the observations. The best fit value of the fraction η_{MT} of MT-BSS with respect to the total number of BSS [i.e. $\eta_{MT} \equiv N_{MT-BSS}/(N_{MT-BSS} + N_{COL-BSS})$, where N_{MT-BSS} and $N_{COL-BSS}$ are the number of mass-transfer and collisional BSS, respectively] is reported in Table 2, as well as the reduced χ^2 of the best fit solution.

In order to determine the best fit solution, we have created a one-dimensional grid of simulations for each cluster, allowing the only free parameter in our model¹, η_{MT} , to vary

¹ Other possible parameters (such as the initial velocity of BSS) were found to have only minor impact on the results (see Section 2) and have been set to a fixed value in all the considered runs. Also, the cluster properties are not free parameters in the fitting procedure, because they have been chosen *a priori* (see Section 3) and kept fixed in all simulations of a given cluster. An exception was made only for the peculiar case of the velocity dispersion in NGC 6752 (see Section 4.3).

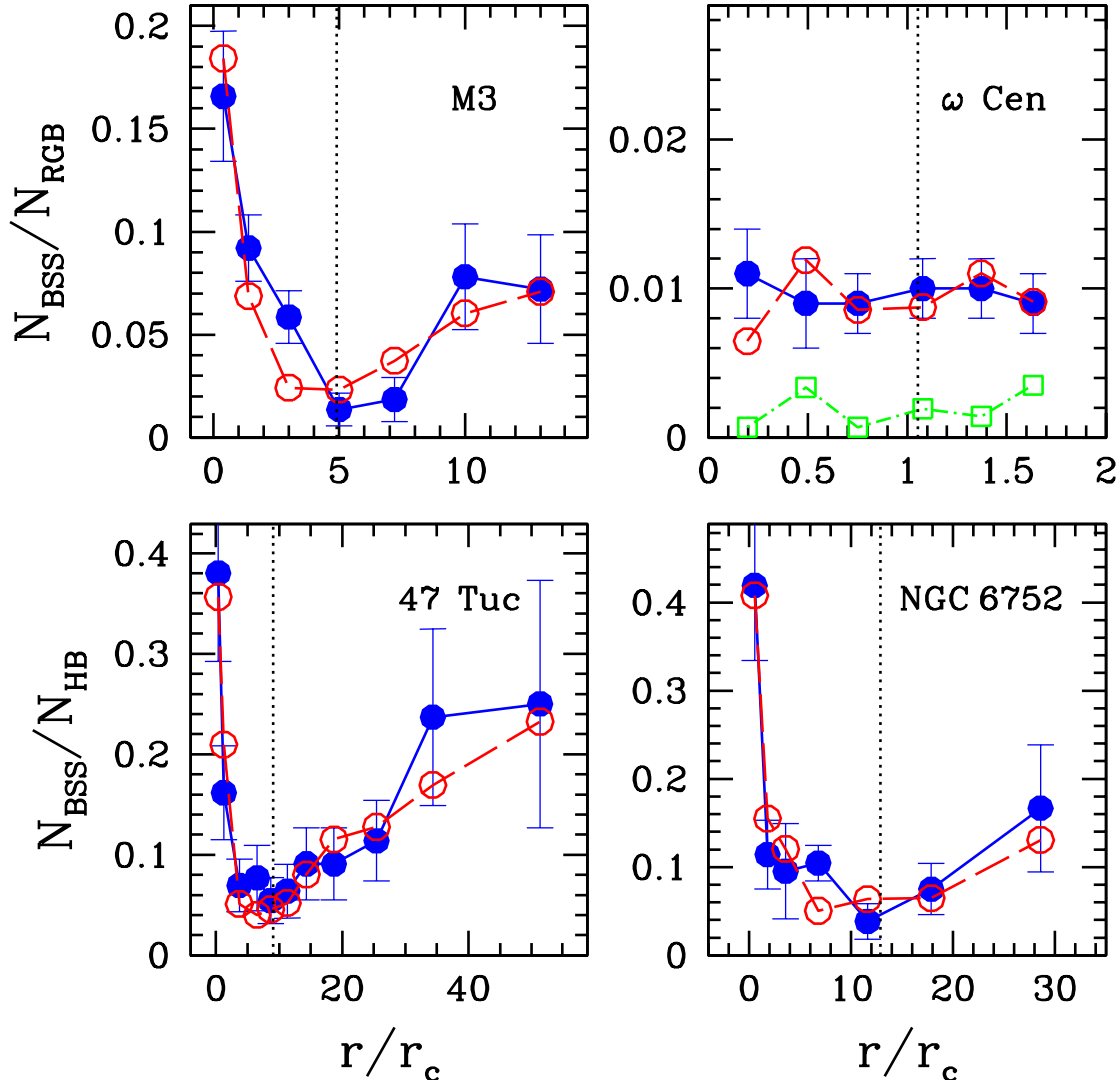


Figure 2. Radial distribution of BSS normalized to the distribution of horizontal branch (HB) stars (47 Tuc, NGC 6752) or red giant branch (RGB) stars (M3, ω Cen). Filled circles and solid lines indicate the data taken from Ferraro et al. 1997a (M3), Ferraro et al. 2006a (ω Cen), Ferraro et al. 2004 (47 Tuc), Sabbi et al. 2004 (NGC 6752). Open circles and dashed lines indicate the best fits obtained from our simulations. For NGC 6752 we adopted $r_c = 28''$ (see text and Table 2). In the panel of ω Cen, the open squares and the dot-dashed line connecting them report the ratio $N_{\text{XMM}}/N_{\text{RGB}}$, that is the number of X-ray sources detected in ω Cen by XMM (Gendre et al. 2003) normalized to the number of RGB stars.

between 0 and 1 with an initial step of 0.2. Then, the grid was iteratively refined down to a step of 0.01 for the values surrounding the best fit.

The values $\tilde{\chi}^2$ of the reduced χ^2 were derived by comparing each simulation with the observed data and their uncertainties. The range of values for η_{MT} in the second column of Table 2 is calculated at $2 - \sigma$ level, *i.e.* by selecting all the simulations for which $\chi^2 \leq \chi^2_{\text{best}} + 4$, where χ^2_{best} is the value for the best fit solution.

Inspection of Table 2 reveals a clear dichotomy between the cases of 47 Tuc, M3 and NGC 6752 and that of ω Cen. The $2 - \sigma$ intervals of confidence for η_{MT} for the first three GCs are in agreement with an almost even distribution of MT-BSS and COL-BSS (a slight predominance of COL-BSS

being indicated by the best fit models). Instead, in the best fit model of ω Cen only 14% of BSS are COL-BSS and the $2 - \sigma$ interval of confidence is compatible with $\eta_{\text{MT}} = 1$.

In the following, we will discuss the case of these three clusters separately, whereas ω Cen will be examined in Section 5.

4.1 M3

In the case of M3, our findings contrast earlier suggestions by Sigurdsson et al. (1994). They hypothesized that the BSS observed in the peripheral regions of M3 could be COL-BSS born initially in the core and then ejected in the periphery because of their natal kick. Indeed, our dynamical simula-

tions show that COL-BSS are ejected from the entire cluster (if the kick is too high), or sink back to the core in $\lesssim 1$ Gyr, if the kick is low enough to retain them in the cluster potential well. Hence, they cannot account for the peripheral BSS. Instead, MT-BSS have in general much more circular orbits than the COL-BSS and can remain in the peripheral regions of the GC for a time comparable to the typical lifetime of a BSS.

4.2 47 Tuc

As for 47 Tuc, we confirm the main outcome from paper I: *i.e.* most of the central BSS of 47 Tuc are born from collisions and all the peripheral BSS originate from mass-transfer in binaries. However, in paper I it was suggested that only $\sim 25\%$ of the total BSS are MT-BSS. The upward correction of this estimate is due to the fact that we have refined our parameter grid with respect to paper I. In paper I we considered only cases with a relatively low fraction of MT-BSS ($\lesssim 30\%$) and one single case with $\eta_{\text{MT}} = 1$. For this paper we explored a more complete parameter space, the percentage of MT-BSS (with respect to the total number of BSS) going from 0 to 100%. Our present best fit (46% MT-BSS and 54% COL-BSS) is still consistent (at $2 - \sigma$) with the result of paper I (25% MT-BSS and 75% COL-BSS), given the observational uncertainties, especially in the central bins (see Fig. 2).

4.3 NGC 6752

The parameters of the best fit model for NGC 6752 are similar to those inferred for M3 and 47 Tuc. However, for this cluster there may be a caveat about the central velocity dispersion, whose value is still very uncertain. From the integrated-light spectra of the core, Dubath et al. (1997) derived $\sigma = 4.9^{+2.4}_{-1.4} \text{ km s}^{-1}$. More recently, from proper motion measurements of a sample of ~ 1000 stars with the WFPC2/HST, Drukier et al. (2003) obtained $\sigma = 12.4 \pm 0.5 \text{ km s}^{-1}$. Thus, we ran simulations for each of these two possibilities.

If we assume $t_{\text{last}} = 1.5$ Gyr, the best fit model obtained for $\sigma = 4.9 \text{ km s}^{-1}$ (Fig. 3) is not satisfactory, since we cannot reproduce the increasing number of BSS located in the cluster outskirts. In fact, a low velocity dispersion implies that the dynamical friction time-scale is too short ($\ll 1$ Gyr) and PBs rapidly shrink towards the core. If we adopt $\sigma = 12.4 \text{ km s}^{-1}$, the rising trend of the BSS radial distribution in the cluster periphery can be reproduced; but the $\tilde{\chi}^2$ (~ 5) is still unacceptable, because of the disagreement with the data points in the inner regions. Since none of the two options were satisfying, we ran new simulations for other values of σ (ranging between 4.9 and 12.4 km s^{-1}), until we found an acceptable fit to the observed BSS distribution. That occurs for $\sigma = 7^{+3}_{-1} \text{ km s}^{-1}$ ($\tilde{\chi}^2 = 1.7$, reported in Table 2), marginally consistent with the measurement of Dubath et al. (1997).

However, for this cluster other marginally acceptable solutions for the BSS radial profile exist: *e.g.* assuming $t_{\text{last}} = 4$ Gyr, a fit ($\tilde{\chi}^2 \lesssim 3$) can be obtained also for $\sigma = 12.4 \text{ km s}^{-1}$ (open triangles and short-dashed line in Fig. 3). Considering this uncertainty and the peculiarities of NGC 6752 (*e.g.* the

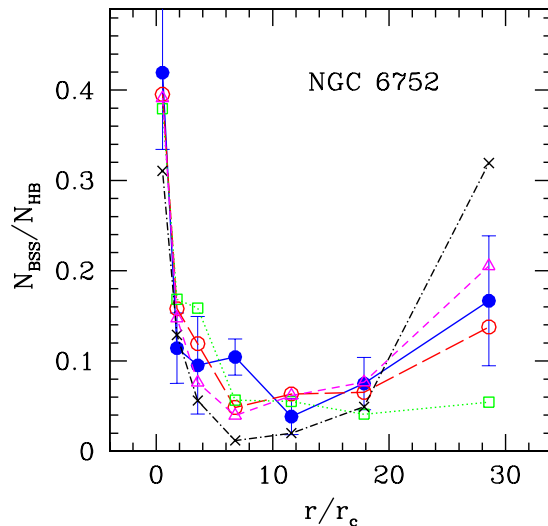


Figure 3. Distribution of BSS normalized to the distribution of HB stars in NGC 6752. The solid line indicates the observations (filled circles; Sabbi et al. 2004). The dotted line (connecting open squares) reports the best fit numerical simulation for $\sigma = 4.9 \text{ km s}^{-1}$; the long-dashed line (connecting open circles) is for $\sigma = 7 \text{ km s}^{-1}$ (reported also in Fig. 2); the dot-dashed line (connecting crosses) is for the case $\sigma = 12.4 \text{ km s}^{-1}$. In all these cases $t_{\text{last}} = 1.5$ Gyr. The short-dashed line connecting open triangles is obtained for $\sigma = 12.4 \text{ km s}^{-1}$ and $t_{\text{last}} = 4$ Gyr.

unusual density profile), the aforementioned best fit value $\sigma = 7^{+3}_{-1} \text{ km s}^{-1}$ cannot be taken as an indirect measurement of the central velocity dispersion in the cluster. A new measurement of σ is strongly needed to understand the dynamics and evolution of NGC 6752.

4.4 The location of the minimum in the BSS radial distributions

The radial distribution of BSS (normalized to the number of RGB or HB stars) in M3, 47 Tuc, and NGC 6752 clearly displays a minimum at a distance from the cluster center in the range $5 - 10 r_c$. The area surrounding this minimum was dubbed "zone of avoidance" (paper I). We expect that its location roughly corresponds to the radius r_{av} below which all the PBs of mass $\gtrsim m_{\text{BSS}}$ (where m_{BSS} is the minimum mass for generating BSS via mass-transfer) have already sunk towards the cluster center because of dynamical friction. In other words, there is a small probability of observing a MT-BSS located at a distance from the cluster center of the order of r_{av} . Most likely, the MT-BSS which were originally located at $r \lesssim r_{\text{av}}$ can now be detected at $r \lesssim r_c$.

The time of dynamical friction t_{df} for a mass m_{BSS} located at a radius r from the center of a GC is given by (Binney & Tremaine 1987)

$$t_{\text{df}} = \frac{3}{4 \ln \Lambda G^2 (2\pi)^{1/2}} \frac{\sigma(r)^3}{m_{\text{BSS}} \rho(r)}, \quad (1)$$

where $\ln \Lambda \sim 10$ is the Coulomb logarithm and G the gravitational constant. $\rho(r)$ and $\sigma(r)$ are the cluster density and the velocity dispersion at the radius r . We note the dependence of t_{df} on the density $\rho(r)$ and especially on the cube

Table 2. Mass Transfer vs Collisional Scenario

	η_{MT}	$\eta_{\text{MT}}(< r_c)$	$\eta_{\text{MT}}(> r_{\text{av}})$	$\tilde{\chi}^2$	r_{av}/r_c
NGC 104	$0.46^{+0.06}_{-0.22}$	$0^{+0.002}_{-0}$	$0.95^{+0.02}_{-0.10}$	0.5	9.0
NGC 5272	$0.41^{+0.16}_{-0.20}$	$0^{+0.002}_{-0}$	$0.91^{+0.02}_{-0.01}$	2.2	4.9
NGC 6752	$0.41^{+0.12}_{-0.04}$	$0.02^{+0.03}_{-0.02}$	$0.97^{+0.01}_{-0.05}$	1.7	12.9
NGC 5139	$0.86^{+0.14}_{-0.08}$	$0.64^{+0.36}_{-0.04}$	$0.90^{+0.10}_{-0.002}$	0.8	1.05

The second column reports the fraction η_{MT} of MT-BSS with respect to the total number of BSS (the errors are at $2-\sigma$, *i.e.* referred to $\chi^2 = \chi^2_{\text{best}} + 4$). The third (fourth) column reports the fraction of MT-BSS inside r_c (outside r_{av}) with respect to the total number of BSS inside r_c (outside r_{av}). The fifth column lists the reduced χ^2 obtained for the best fit models. The rightmost column reports r_{av} normalized to r_c .

of the velocity dispersion. Given the definition of this time-scale, r_{av} can be calculated setting $t_{\text{df}} = t_{\text{gc}}$, where t_{gc} is the lifetime of the cluster (~ 12 Gyr), and using the simulated stellar density profile and the velocity dispersion distribution of the cluster for inferring r_{av} from $\rho(r_{\text{av}})$ and $\sigma(r_{\text{av}})$. In doing the calculation, we choose $m_{\text{BSS}} = 1.2 M_{\odot}$.

The results (for r_{av} normalized to r_c) are shown in the last column of Table 2 and in Fig. 2 (vertical dotted line). The values of r_{av} are always consistent with the zone of avoidance observed in the data. This confirms for M3 and NGC 6752 what had been found for 47 Tuc (paper I).

Third and fourth columns of Table 2 report the values of the fraction η_{MT} (*i*) for the MT-BSS located within the GC core r_c ($\eta_{\text{MT}}(< r_c)$), and (*ii*) for the MT-BSS found at a distance from the cluster center larger than r_{av} ($\eta_{\text{MT}}(> r_{\text{av}})$). These findings indicate that the position of a BSS in a GC (at least in those showing a bimodal distribution of the BSS) can be used as a strong indication of the nature of the progenitor. In particular, a BSS which is located outside the zone of avoidance almost certainly is a MT-MSS; on the contrary, a BSS found close to the cluster core is a COL-BSS.

Among the considered clusters, only ω Cen does not show any zone of avoidance. If we calculate the expected radius of avoidance also for this cluster, we find $r_{\text{av}} \sim r_c$. This indicates that in ω Cen the dynamical friction is far less efficient than in the other clusters. In ω Cen the value of $\eta_{\text{MT}}(> r_{\text{av}})$ is similar to the other clusters, whereas $\eta_{\text{MT}}(< r_c)$ is much higher (see Section 5).

We note that very similar values of both η_{MT} and r_{av}/r_c have been obtained for an intermediate density GC (M3) and for two much denser clusters (47 Tuc and NGC 6752). The analogy between these three clusters is even more evident in Fig. 4, where radial distances are normalized to the avoidance radius, r_{av} . The radial distributions of BSS in M3, 47 Tuc and NGC 6752 nearly superimpose. This also indicates that r_{av} is a crucial parameter in describing the bimodal distribution of BSS.

5 THE CASE OF ω CENTAURI

The main characteristic of the BSS radial distribution of ω Cen, with respect to the other clusters discussed here, is

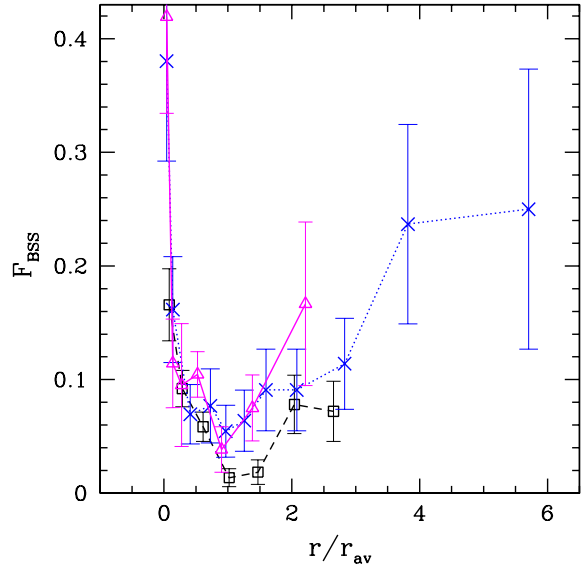


Figure 4. Observed distribution of BSS normalized to the distribution of HB (47 Tuc, NGC 6752) or RGB stars (M3). On the x-axis we plot the distance from the center normalized to r_{av} . Crosses indicate the observational data for 47 Tuc, open squares for M3 and open triangles for NGC 6752. The observational points are connected by a dashed line for M3, a dotted line for 47 Tuc and a solid line for NGC 6752.

the absence of any central peak. In Fig. 2 we show the high-resolution portion of the data-set presented by Ferraro et al. (2006a): the distribution appears to be flat. This is quite unusual, since in all the other GC surveyed up to now the BSS distribution is peaked at the cluster center. Fig. 6 by Ferraro et al. (2006a) suggests that this behaviour extends up to at least $\sim 7 r_c$ ($\sim 20'$ from the cluster center).

This peculiarity adds to the many other unique features displayed by ω Cen (see Section 3); but our simple model provides a satisfactory fit to the data (see Fig. 2 and Table 2) also in this case. However, at variance with the results for the three clusters examined in Section 4, the best fit model requires that a large majority of the BSS are born from PBs (see Table 2). In other words, only a mere $\sim 14\%$ of the BSS detected in ω Cen may have a collisional origin, *i.e.* we expect that only ~ 44 of the 313 BSS reported by Ferraro et al. (2006a) are COL-BSS.

The alternative hypothesis that all the others BSS formed via collisions have been ejected from ω Cen sounds unrealistic, since the central escape velocity of ω Cen ($\sim 40 \text{ km s}^{-1}$) is comparable with that of other clusters in our sample and there is no motivation for assuming that collisions in ω Cen should generate larger recoil velocities with respect to other clusters. As a consequence, the dynamical modeling of the BSS presented in this work predicts that COL-BSS are now produced with a low rate in ω Cen.

Are there viable explanations for this underproduction of COL-BSS in ω Cen? We can just note that the characteristic radius r_{av} for ω Cen is much smaller (both in terms of r_c and of physical units) than in the other clusters of our sample ($r_{\text{av}} \sim r_c$ instead of the typical value ranging between $5 r_c$ and $15 r_c$). This means that only a small number

of PBs had enough time to sink into the core due to mass segregation.

PBs that sink within the core are thought to be the progenitors (as far as modified by three body interactions) of most of the binaries hosted in the core of current GCs, since the formation of binaries from two-body interactions is a quite unlikely process. Because of their large cross-section, core binaries suffer repeated three- and four-body interactions, eventually exchanging companions, being ionized or hardened. Thus, core binaries are required to form COL-BSS, via three- or four-body encounters. Then, the relative lack of binaries in the core of ω Cen, due to the inefficiency of dynamical friction, could have quenched the formation of COL-BSS.

This view could be strongly supported by the observation of a low ($\ll 10\%$) fraction of binaries in the core of ω Cen. Unfortunately, this fraction cannot be derived with classical methods (Rubenstein & Bailyn 1997; Bellazzini et al. 2002), because of the wide spread in metallicity of the stars in this GC (Norris et al. 1996; Suntzeff & Kraft 1996). An indirect indication of the occurrence of a low fraction of binaries in the core of ω Cen comes from inspection of Fig. 2, which shows the radial distribution of the X-ray sources observed in ω Cen by XMM (Gendre et al. 2003), normalized to the number of RGB stars. Most of the X-ray sources are believed to be cataclysmic variables or low mass X-ray binaries (Gendre et al. 2003). So they should be among the most massive objects in the GC. Their flat radial distribution further supports the hypothesis that mass segregation in ω Cen has not driven yet a sizeable number of massive binaries in the central region.

6 NUMBER OF BSS VERSUS M_V

Until now, we only considered the relative frequency of BSS, *i.e.* the number of BSS normalized to that of HB and/or RGB stars. But what happens if we consider just the number of BSS hosted in each cluster, without any normalization?

First of all, it is worth noting that NGC 6752 (ω Cen) hosts about three times fewer (more) BSS than either 47 Tuc or M3 (Fig. 5). We can ask whether this is at all correlated to the mass of the host cluster, or, equivalently, to its absolute magnitude M_V ? Plotting in Fig. 5 the total number of observed BSS per cluster against M_V for our four clusters, we do not see any straight correlation. This result agrees with the fact that Piotto et al. (2004) found evidence, in a large sample of GCs, of a lack of correlation of the number of observed BSS with either stellar collision rate (as would be expected if all BSS were collisional in origin) or mass (which is proportional to the collision rate).

This fact led Davies et al. (2004) to propose that BSS are made through both channels, suggesting that the number of COL-BSS tends to increase with cluster mass, while MT-BSS tend to decrease with total mass, as PBs drifting by dynamical friction in the core had already time to burn as BSS in the past. The combination of these two competing behaviours was found to produce a population of BSS weakly dependent on the total mass and core collision rate of their host GC.

Fig. 5 sketches the predictions by Davies et al. (2004). In particular, the dashed (dotted) line indicates the contribution

expected from the MT- (COL-)BSS; the solid line is the total.

47 Tuc and M3 lie close to the solid line and, according to the Davies et al.'s model, their current BSS population is obtained by a blending of COL-BSS and MT-BSS contributing in roughly equal number. This fully agrees with what we found from the comparison between our simulations and the radial distribution of BSS.

In contrast, our model and Davies et al.'s scenario disagree in the case of both NGC 6752 and ω Cen. NGC 6752 lies well below the solid curve. According to Davies et al. (2004), its BSS should predominantly be MT-BSS; whereas in our model NGC 6752 should host MT-BSS and COL-BSS nearly in equal number. In the Davies et al.'s model ω Cen is expected to have only COL-BSS, while we have shown that MT-BSS should dominate².

Moreover, though the picture proposed by Davies et al. (2004) is interesting, detailed cluster-to-cluster comparisons suggest a much more complex scenario, where the dynamical history, the original PB content and the current dynamical state of each cluster seem to play a major role (Ferraro et al. 2003a). Indeed, clusters with the same integrated magnitude harbor quite different BSS populations. In particular, two GC pairs offer the possibility of demonstrating the complexity of the emerging scenario: (i) M3 and M13 are almost twins GCs (Ferraro et al. 1997b). They have the same integrated magnitude ($M_V \sim -8.6$), same metallicity ($[Fe/H] = -1.6$), same mass, but display a quite different BSS content (Ferraro et al. 2003a). In particular, M13 harbors a factor 5 fewer BSS than M3. (ii) NGC 6752 has an integrated magnitude ($M_V \sim -7.7$) which is quite similar to M80 ($M_V \sim -7.9$); but again the BSS content in the two clusters turns out to be quite different: NGC 6752 harbors a BSS population which is a factor 10 lower than that found in M80 (note that the BSS population of M80 is comparable in size to that found in ω Cen). Ferraro et al. (1999) suggested that the anomalously large population of BSS in M80 could have originated in the core-collapsing phase of this cluster.

The model discussed in this paper is based on a different approach from that of Davies et al. (2004). Neither this work nor Davies et al.'s accounts for the dynamical evolution of the cluster; but we consider additional information in comparison with Davies et al. (2004), *i.e.* the observed BSS radial distribution.

Davies et al. (2004) try to predict the properties of the BSS from the present properties of the host cluster, and these properties might not reflect all the stages in the cluster evolution. In particular, they risk overlooking the importance of the earlier evolutionary phases which can have a strong impact on the characteristics of BSS population.

In our approach the cluster evolution is frozen for the last 2 Gyr only, when the cluster properties are not expected to have changed significantly. All the effects of the previous evolution of the cluster onto BSS are intrinsically stored in the initial parameters which we impose on the BSS population: masses, lifetimes, velocities, locations and the amount of injected MT-BSS and COL-BSS. Hence, we can use the observed BSS radial profile for inferring the ratio between

² Davies et al. (2004) admit that their model is not adaptable to slow evolving GCs like ω Cen.

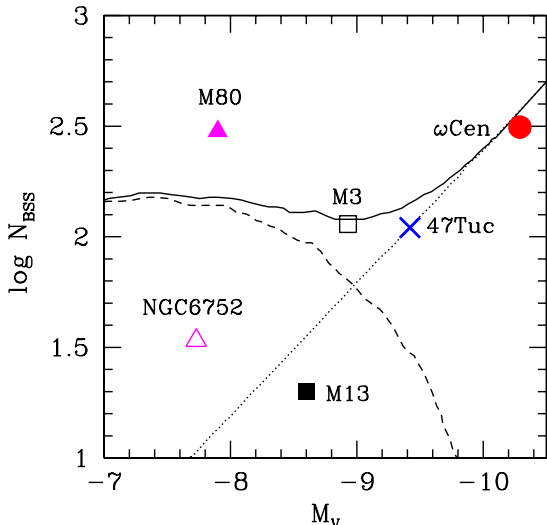


Figure 5. Number of BSS as a function of the cluster absolute magnitude M_V . Open triangle refers to NGC 6752, filled triangle to M80, open square to M3, filled square to M13, cross to 47 Tuc, filled circle to ω Cen. The values of M_V come from the Harris catalogue (Harris 1996; <http://physwww.mcmaster.ca/%7Eharris/mwgc.dat>). The solid line shows the model by Davies et al. (2004), while the dashed (dotted) line refers to the MT-BSS (COL-BSS) according to the same model.

the injected MT-BSS and COL-BSS (which is related to their location), and for investigating the effects of the cluster (present) properties on that (*e.g.* what is the importance of collisions in the recent life of the cluster; and, what is the residual fraction of PBs needed to remain in periphery up to now).

Both these methods need refinements; however, the approach presented in this paper has the advantage that it is able to fit the BSS population also in clusters where Davies et al.'s method appears inaccurate. A complete understanding of the relation between a cluster and its BSS population will likely be possible only by running N-body simulations of the cluster from its formation, accounting also for three-body encounters, PB evolution, stellar evolution, etc.

7 SUMMARY

We have exploited the recent determination of the radial distribution of BSS in four GCs, in order to investigate which mechanism of BSS formation prevails in these stellar systems. Our conclusion is that the two main formation paths proposed so far, *i.e.* mass-transfer in PBs and merging of MS stars due to collisions in the cluster core, must *coexist and have similar efficiency both in a low density cluster (M3) and in much denser clusters, like 47 Tuc and NGC 6752*.

In particular, in M3, 47 Tuc, and NGC 6752 the COL-BSS sum to $\sim 50 - 60\%$ of the total and mostly reside in the central region of the cluster. The MT-BSS are slightly less abundant than the COL-BSS, but populate all the GC. The density of BSS reaches a minimum in a so-called zone of avoidance, which separates the portion of the GC mostly

occupied by COL-BSS from the cluster outskirts, where the MT-BSS dominate. The location of the zone of avoidance is explained by accounting for the effects of the dynamical friction on the PBs which were massive enough for generating the observed BSS.

The picture described above can also be applied to ω Cen; but in this case the lack of a central peak in the BSS radial distribution requires that the large majority of the BSS derive from PBs. The very low rate of production of COL-BSS could be in turn attributed to the fact that mass segregation has not yet driven a sizeable number of PBs to the central region of the cluster to produce BSS.

A very interesting further development of this research will be to perform a comparison between the location of a significant sample of BSS in a GC and their spectroscopic properties. According to the findings of this work, the position in the GC might represent a strong dynamical clue for the formation mechanism of a given BSS. If it is located outside the zone of avoidance, the BSS almost certainly results from evolution of a PB; if it is harbored in the cluster core, the BSS has most likely a collisional origin. On the other hand, indication about the origin of the same BSS can be independently obtained from high resolution spectroscopy. Indeed the chemical signature of the MT-BSS formation process has been recently discovered in 47 Tuc (Ferraro et al. 2006b). The acquisition of similar sets of data in clusters with different structural parameters and/or in different regions of the same cluster will provide an unprecedented tool for confirming the scenario presented here and to finally address the BSS formation processes and their complex interplay with the dynamical evolution of the cluster.

8 ACKNOWLEDGMENTS

We thank Craig Heinke, Fred Rasio and Emanuele Ripamonti for useful discussions. We acknowledge the anonymous Referee for the critical reading of the manuscript. M. M. acknowledges the Northwestern University and the Center for Gravitational Wave Physics (Pennsylvania State University) for kind hospitality. M. C. and A. P. acknowledge grant PRIN05 2005024090_002. This research was supported by the contract ASI-INAF I/023/05/0.

REFERENCES

- Bailyn C. D., 1995, *ARA&A*, 33, 133
- Bailyn C. D., & Pinsonneault M. H., 1995, *ApJ*, 439, 705
- Beccari, G., Ferraro, F.R., Possenti, A., Valenti, E., Origlia, L., Rood, R.T., 1996, *AJ*, 131, 2551
- Bellazzini M., Ferraro F. R., Sollima A., Pancino E., Origlia L., 2004, *A&A*, 424, 199
- Bellazzini M., Fusi Pecci F., Messineo M., Monaco L., Rood R. T., 2002, *AJ*, 123, 1509
- Binney J., Tremaine S., 1987, *Galactic Dynamics* (Princeton: Princeton Univ. Press)
- Carney B. W., Latham D. W., Laird J. B., Grant C. E., Morse J. A., 2001, *AJ*, 122, 3419
- Colpi M., Mapelli M., Possenti A., 2003, *ApJ*, 599, 1260
- D'Amico N., et al., 2002, *ApJ*, 570, L89
- Davies M. B., Benz W., Hills J. G., 1994, *ApJ*, 424, 870
- Davies M. B., Piotto G., De Angeli F., 2004, *MNRAS*, 349, 129

Drukier G. A., Bailyn C. D., Van Altena W. F., Girard T. M., 2003, AJ, 125, 2559

Dubath P., Meylan G., Mayor M., 1997, A&A, 324, 505

Ferraro F. R. et al., 2006b, ApJ, 647, L53

Ferraro F. R., Beccari G., Rood R. T., Bellazzini M., Sills A., Sabbi E., 2004, ApJ, 603, 127

Ferraro F. R., Carretta E., Corsi C. E., Fusi Pecci F., Cacciari C., Buonanno R., Paltrinieri B., Hamilton D., 1997a, A&A, 320, 757

Ferraro F. R., Fusi Pecci F., Cacciari C., Corsi C., Buonanno R., Fahlman G. G., Richer H. B., 1993, AJ, 106, 2324

Ferraro F. R., Messineo, M., Fusi Pecci F., De Palo, M.A., Straniero, O., Chieffi, A., Limongi, M., 1999, AJ, 118, 1738

Ferraro F. R., Paltrinieri, B., Fusi Pecci, F., Cacciari, C., Dorman, B., rood, R.T., 1997b, ApJ, 484, L145

Ferraro F. R., Possenti A., Sabbi E., Lagani P., Rood R. T., D'Amico N., Origlia L., 2003b, ApJ, 595, 179

Ferraro F. R., Sills A., Rood R. T., Paltrinieri B., Buonanno R., 2003a, ApJ, 588, 464

Ferraro F. R., Sollima A., Rood R. T., Origlia L., Pancino E., Bellazzini M., 2006a, ApJ, 638, 433

Freeman K. C., 1993, The globular clusters-galaxy connection. Astronomical Society of the Pacific Conference Series, Volume 48, Proceedings of the 11th Santa Cruz Summer Workshop in Astronomy and Astrophysics, held July 19-29, 1992, at the University of California, Santa Cruz, San Francisco: Astronomical Society of the Pacific (ASP), edited by Graeme H. Smith, and Jean P. Brodie, 608

Fusi Pecci F., Ferraro F. R., Corsi C. E., Cacciari C., Buonanno R., 1992, AJ, 104, 1831

Gendre B., Barret D., Webb N. A., 2003, A&A, 400, 521

Gilliland R. L., Bono G., Edmonds P. D., Caputo F., Cassisi S., Petro L. D., Saha A., Shara M. M., 1998, ApJ, 507, 818

Harris W.E., 1996, AJ, 112, 1487

Hurley J. R., Tout C. A., Aarseth S. J., Pols O. R., 2001, MNRAS, 323, 630

Ideta M., Makino J., 2004, ApJ, 616L, 107

Ivanova N., Belczynski K., Fregeau J. M., Rasio F. A., 2005, MNRAS, 358, 572

Leonard P. J. T., 1989, AJ, 98, 217

Lombardi J. C. Jr., Warren J. S., Rasio F. A., Sills A., Warren A. R., 2002, ApJ, 568, 939

Mapelli M., Sigurdsson S., Colpi M., Ferraro F. R., Possenti A., Rood R. T., Sills A., Beccari G., 2004, ApJ, 605L, 29

McCrea W. H., 1964, MNRAS, 128, 147

Merritt D., Meylan G., Mayor M., 1997, AJ, 114, 1074

Meylan G., Mayor M., Duquennoy A., Dubath P., 1995, A&A, 303, 761

Monkman E., Sills A., Howell J., Guhathakurta P., de Angeli F., Beccari G., ApJ, accepted

Norris J. E., Freeman K. C., Michell K. J., 1996, ApJ, 462, 241

Piotto G. et al., 2004, ApJ, 604L, 109

Pooley D., et al., 2003, ApJ, 591, L131

Portegies Zwart S. F., Makino J., McMillan S. L. W., Hut P., 1999, A&A, 348, 117

Portegies Zwart S. F., Hut P., Verbunt F., 1997, A&A 328, 130

Proctor Sills A., Bailyn C. D., Demarque P., 1995, ApJ, 455, L163

Pryor C., Meylan G., 1993, Structure and Dynamics of Globular Clusters. Proceedings of a Workshop held in Berkeley, California, July 15-17, 1992, to Honor the 65th Birthday of Ivan King. Editors, S.G. Djorgovski and G. Meylan; Publisher, Astronomical Society of the Pacific, Vol. 50, 357

Reijns R. A., Seitzer P., Arnold R., Freeman K. C., Ingerson T., van den Bosch R. C. E., van de Ven G., de Zeeuw P. T., 2006, A&A, 445, 503

Rey S. C., Lee Y. W., Ree C. H., Joo J. M., Sohn Y. J., Walker A. R., 2004, AJ, 127, 958

Rubenstein E. P., Bailyn C. D., 1997, ApJ, 474, 701

Sabbi E., Ferraro F. R., Sills A., Rood R. T., 2004, ApJ, 617, 1296

Sigurdsson S., Davies M. B., Bolte M., 1994, ApJ, 431, L115

Sigurdsson S., Phinney E. S., 1993, ApJ, 415, 631

Sigurdsson S., Phinney E. S., 1995, ApJS, 99, 609

Sills A., Bailyn C. D., 1999, ApJ, 513, 428

Sills A., Bailyn C. D., Edmonds P. D., Gilliland R. L., 2000, ApJ, 535, 298

Spitzer L., 1987, Dynamical Evolution of Globular Clusters. Princeton Univ. Press

Suntzeff N. B., Kraft R. P., 1996, AJ, 111, 1913

van de Ven G., van den Bosch R. C. E., Verolme E. K., de Zeeuw P. T., 2006, A&A, 445, 513

van Leeuwen F., Le Poole R. S., Reijns R. A., Freeman K. C., de Zeeuw P. T., 2000, A&A, 360, 472

Warren S. R., Sandquist E. L., Bolte M., 2006, submitted, astro-ph/0605047

Zaggia S. R., Piotto G., Capaccioli M., 1997, A&A, 327, 1004

Zinnecker H., Keable C. J., Dunlop J. S., Cannon R. D., Griffiths W. K., 1988, The Harlow Shapley Symposium on Globular Cluster Systems in Galaxies. Proceedings of the 126th Symposium of the International Astronomical Union, held in Cambridge, Massachusetts, U.S.A. August 25-29, 1986. Edited by Jonathan E. Grindlay and A. G. Davis Philip. Kluwer Academic Publishers, Dordrecht, 603